

Chapter 5

RF CHARACTERISTICS OF QWITT DEVICES

In this chapter we will discuss microwave and millimeter wave characteristics of different (QWITT) diode oscillators and self-oscillating mixers. Waveguide and planar circuit implementations of both the oscillator and mixer circuits are presented.

5.1 Microwave and Millimeter Wave QWITT Diode Oscillator

Microwave and millimeter wave waveguide oscillators were implemented using the QWITT devices studied in the previous chapter. The devices were mounted in WR-90 (8-12 GHz) and WR-22 (33-50 GHz) waveguides using a micrometer-controlled post and whisker-contacted for microwave and millimeter-wave measurements. A block diagram of the waveguide oscillator measurement set up is shown in Fig. 5.1. On one end of the waveguide a sliding short is used to modulate the impedance of the waveguide circuit to obtain the highest output power. On the other end the waveguide is coupled to a spectrum analyzer or power meter. DC bias to the diode is provided through a bias-tee to obtain dc and rf isolation. Fig. 5.2 shows a WR-10 waveguide, a GaAs chip containing QWITT diodes of varying diameters mounted on a micrometer controlled post, and a diode whisker contact. In addition, a planar microstrip oscillator circuit was designed using a standard microwave CAD package, Touchstone, to match the QWITT diode impedance

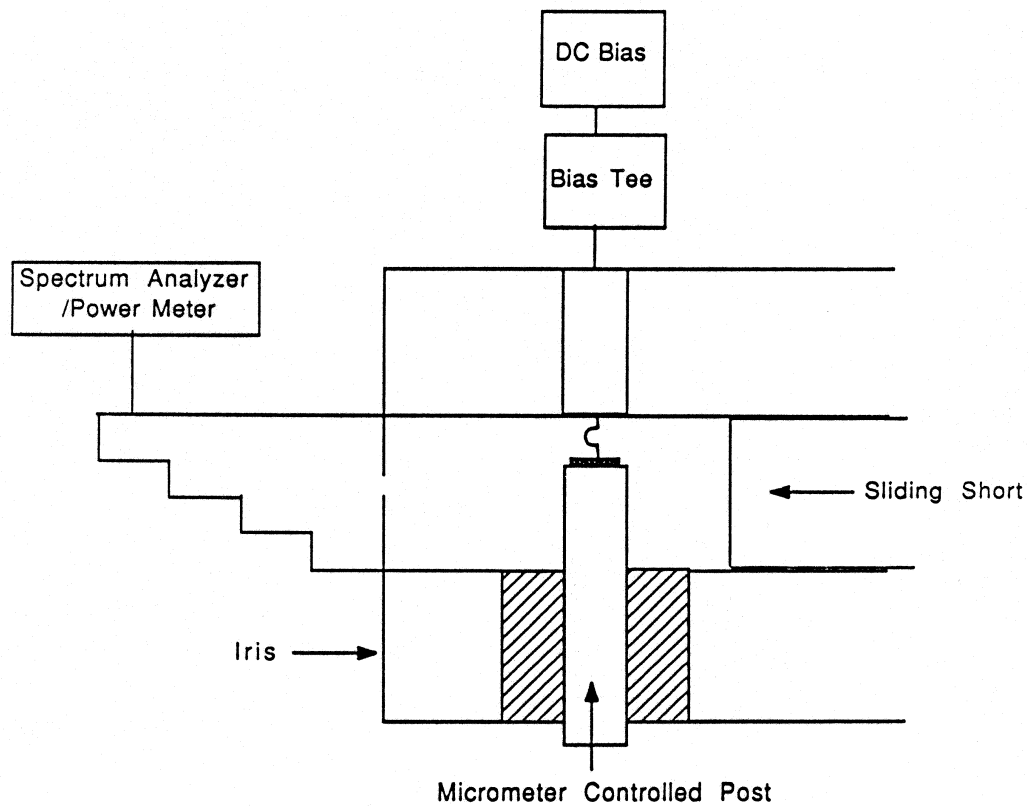


Fig. 5.1: Block diagram of the waveguide circuit used at microwave and millimeter wave frequencies.

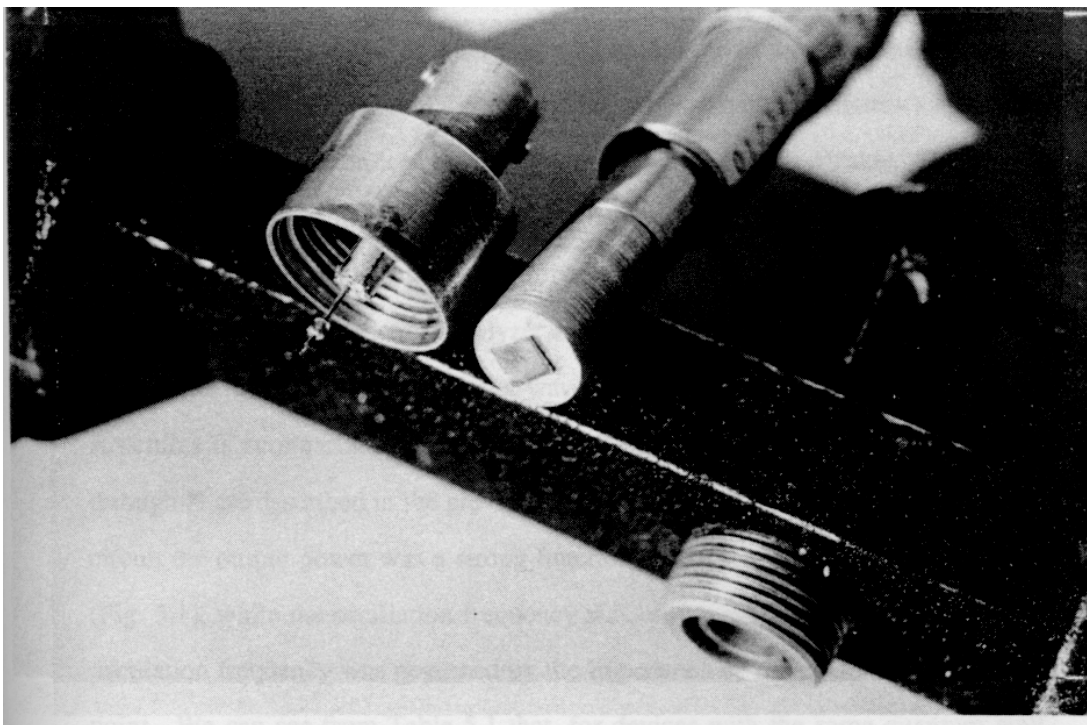


Fig. 5.2: Photograph of a WR-10 waveguide, a GaAs chip containing QWITT diodes of varying diameters mounted on a micrometer controlled post, and a diode whisker contact.

as predicted by the large signal model [66]. Fig. 5.3 shows a photograph of the 10 GHz planar microstrip oscillator used. A lo-hi-lo impedance transformer was used to bias the diode and obtain dc and rf isolation at the bias point. Chip capacitors were used to block the dc signal at the rf output. Fig. 5.4 shows a more detailed view of the QWITT diode chip containing devices with varying diameters (a distinct diffraction pattern can be seen on the chip) contacted by a small whisker. This circuit (Fig. 5.3) represents the first planar implementation of a quantum well oscillator. The output power measurements for the QWITT oscillator were verified independently using a spectrum analyzer and an rf power meter.

The microwave and millimeter-wave performance of different QWITT device structures is summarized in Tables 5.1&5.2. Details of the device structures A through H are described in the previous chapter. For each device in the waveguide circuit the output power was a strong function of the position of the sliding short (Fig. 5.1), while the oscillation frequency was only weakly dependent on it. The oscillation frequency was governed by the impedance of the diode and the dc bias point. We can see from Table 5.1 that, for devices with the same quantum well structure, as the length of the drift region is increased from 500Å to 2000Å, the output power in the waveguide circuit increases from 3 μ W to 30 μ W. The devices were also mounted in a 50 Ω planar microstrip circuit and a coaxial triple stub tuner was used to improve matching between the microstrip circuit and 50 Ω characteristic impedance measurement instruments. With the microstrip circuit oscillations in the frequency range of 5-8 GHz were detected, with a peak output power of \cong 1 mW from device C. The impedance of the planar oscillator circuit is much lower than the waveguide circuit, and the improvement in output power seen in the planar circuit is

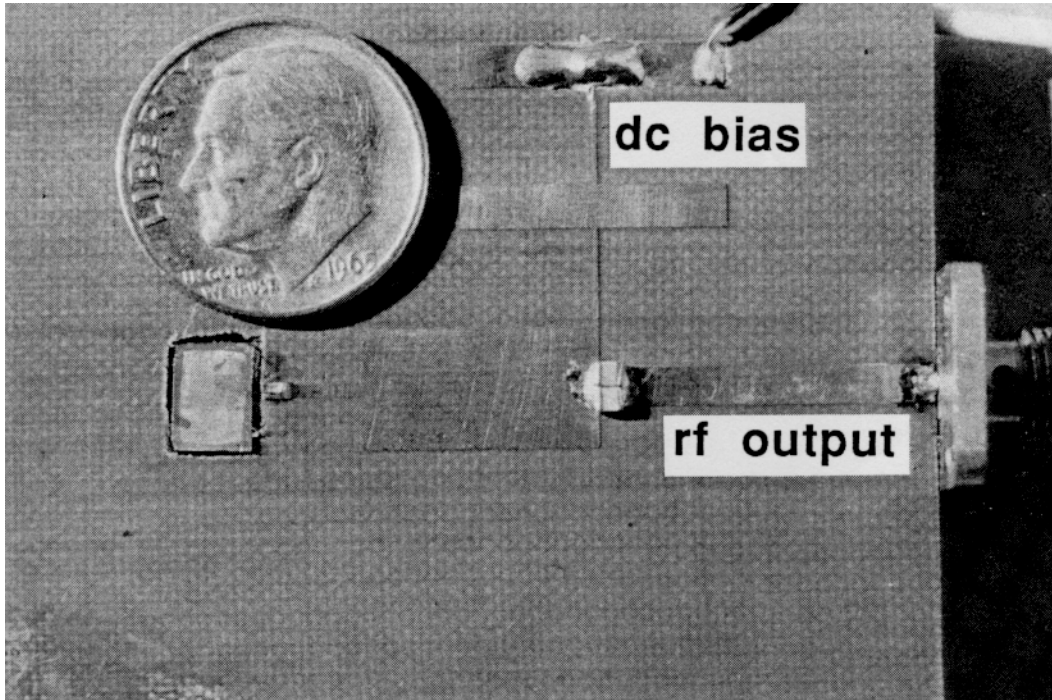


Fig. 5.3: A planar microstrip QWITT diode oscillator at X-band.

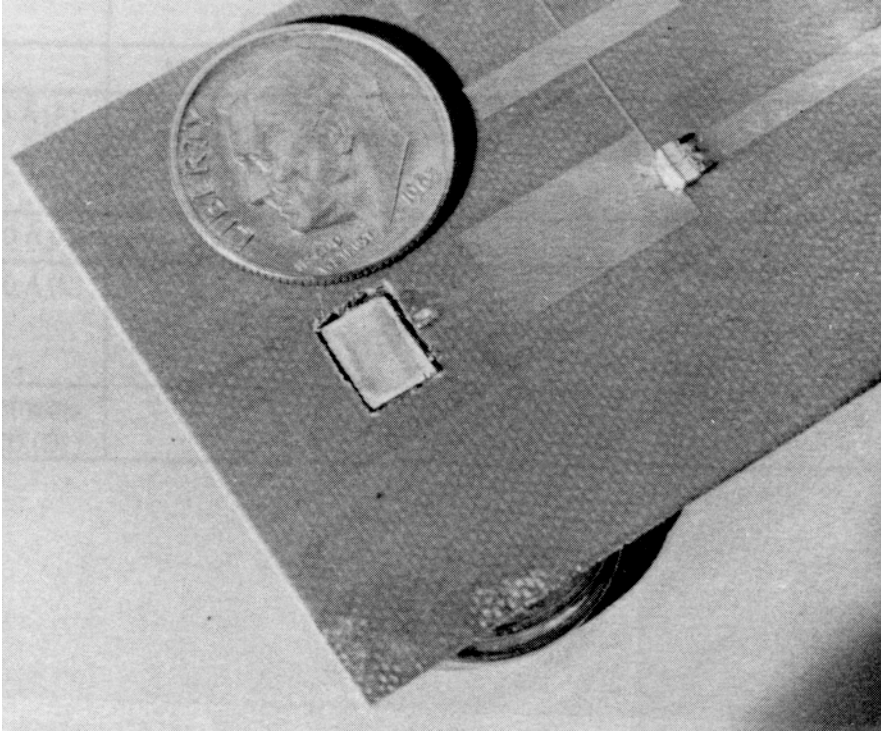


Fig. 5.4: Close up view of the diode chip showing devices of various diameters contacted by a whisker in the planar microstrip circuit.

Drift Region Length	Specific Negative Resistance ($10^{-5} \Omega\text{-cm}^2$)		Output Power (μW)	Oscillation Frequency (GHz)
	Measured	Simulation		
500 Å (A)	2.6	2.4	3 240 (planar) 275 (planar)	8-12 6-8 6-8
1000 Å (B)	3.9	3.7	10	8-12
2000 Å (C)	6.8	5.9	30 30 910 (planar)	8-12 28-31 6-8
Symmetric RTD (D)	3.1	2.7	1	8-12

Table 5.1: Microwave and millimeter-wave performance of QWITT diode oscillators, A through D, in both waveguide and planar circuits.

Doping Spike	Output Power (μW)	Efficiency ($P_{\text{rf}}/P_{\text{dc}}$)	Oscillation Frequency (GHz)
uniform 5×10^{16} (E)	850	3.5%	5 - 8
8×10^{16} (F)	1000	5.0%	5 - 8
1×10^{17} (G)	350	4.3%	5 - 8
5×10^{17} (H)	100	3%	5 - 8

Table 5.2: Microwave performance of QWITT diode oscillators, E through H, in a planar microstrip circuit.

probably due to a better match to the low impedance of the device. For the different devices, as the length of the drift region is increased from 500Å to 2000Å, the output power increases dramatically in both waveguide and planar oscillator circuits (Table 5.1). The output power at 10 GHz is lower than estimates based on large-signal models for the QWITT diode [66, 76]. This is primarily because the device areas used in this study were not optimized to obtain highest output power [66] to avoid excessive heating and consequent heat sinking problems. In Chapter 2 we obtained the optimum device area (see Fig. 2.8) for 10 GHz operation to be around 10^{-3} cm². The device areas used in this study were smaller than this optimum by four orders of magnitude. The peak current density in these devices (Table 4.1) is around 25 kA/cm². By appropriately choosing the thickness of the quantum well layers the current density can be increased further [91], thus improving the device output power. However, the dramatic increase in output power obtained in devices B and C, clearly suggests that, as predicted by the small signal analysis, the intrinsic device specific negative resistance has been increased through an appropriate choice of drift region length. Further, Table 5.1 also shows that at 10 GHz the improvement in rf output power clearly tracks the dc specific negative resistance of the device. This is in keeping with predicted models for the QWITT diode [65] which indicate that the dc I-V curve for the device is a good measure of rf performance at frequencies below $\sigma/2\pi\epsilon$ (typically around 40 GHz). Millimeter wave oscillations in the frequency range 28-31 GHz were obtained in a full-height waveguide circuit from device C with 30 μ W output power (Fig. 5.5). Note that the output power in the WR-22 waveguide circuit at these frequencies (Ka-band) is the same as that obtained from the device in the WR-90 waveguide circuit at X-band. This indicates that the specific

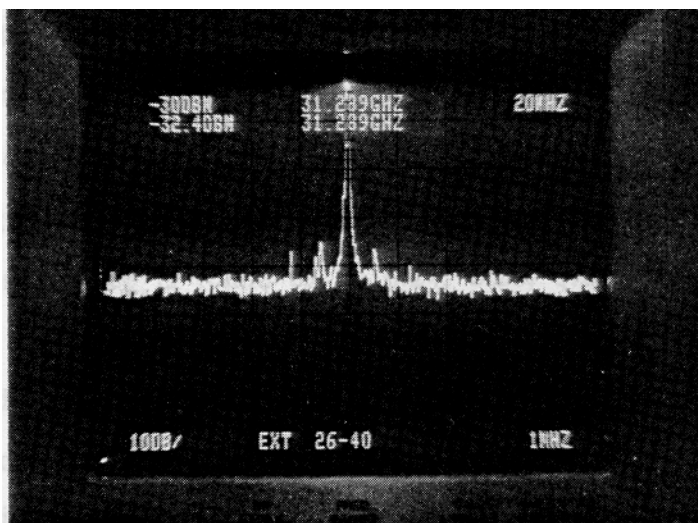


Fig. 5.5: Spectrum of a QWITT diode (device F) oscillating at 31 GHz in a waveguide circuit.

negative resistance of the device is essentially constant from dc to millimeter wave frequencies. This is in keeping with the small signal analysis which predicts a flat response in specific negative resistance at frequencies below $\sigma/2\pi\epsilon$, beyond which the specific negative resistance rolls off as the quantum well capacitance starts to dominate current injection into the drift region.

In order to calculate the specific negative resistance for these devices, the intrinsic injection conductance ($\sigma=\partial J/\partial E$) of the quantum well is determined from the experimental dc I-V characteristics by accounting for the accumulation and depletion regions using a drift/diffusion formalism [74]. For the samples, A, B, C, and D the injection conductance is found to be 0.24, 0.28, 0.20, and 0.15 mho/cm respectively. This value for σ is then used to predict the specific negative resistance for the three devices [65] by assuming a constant carrier velocity in the drift region of 2×10^7 cm/sec (Table. 5.1). We can see from Table 5.1 that the measured specific negative resistance ($\Delta V/\Delta J$) obtained from the dc characteristics of the diode compares well with the predicted small signal simulation results at 10 GHz.

In devices E through H (see Fig. 4.3) a doping spike was introduced at the beginning of the drift region to reduce the electric field and thus decrease the dc bias, but yet fully deplete the entire drift region. The dc characteristics for these devices is shown in Table 4.1 in the previous chapter. We can see that in devices G and H the doping concentration in the spike is so high that a large fraction of the drift region is not depleted, causing a reduction in the voltage swing, ΔV_{pv} . This directly translates into lower rf output power for devices G and H as seen in Table 5.2. Device D, which is the limiting case of the spike (i.e., a uniformly doped drift region) produces an output power of 850 μ W at 3.5% efficiency (Table 5.2). Device

F is clearly the optimum device since by introducing a $8 \times 10^{16} \text{ cm}^{-3}$ doping spike the device efficiency is increased by almost 50% compared to device E, with marginally higher output power (1 mW). The rf results obtained from devices C, E, and F represent significant improvements in output power density over previous reports in the literature [20, 77]. Millimeter wave oscillations in the frequency range 28-31 GHz were also obtained in a full-height waveguide circuit from both devices E and F with 30 μW output power. As before, the output power in the waveguide circuit compared to the microstrip circuit is low due to the poor impedance match between the diode and full height waveguide.

5.2 Self Oscillating QWITT Diode Mixer

There is increasing interest in developing quantum well (QW) devices for millimeter wave technology beyond source applications [78]. Since the primary application for the QWITT diode may be as a local oscillator for a microwave mixer, it may be very advantageous to combine both functions into a single component, as in a self-oscillating mixer. Since the QWITT diode is a highly nonlinear negative resistance device, and due to the fact that quantum mechanical tunneling is an intrinsically low noise phenomenon, self oscillating QWITT diode mixers could be expected to possess some conversion gain and a low noise figure. Therefore, the QWITT diode has the potential of being used as a self oscillating mixer. In this chapter experimental results using the QWITT diode as a waveguide self oscillating harmonic mixer and also as a planar self oscillating mixer operating in the fundamental mode are presented [79, 80].

A schematic diagram of the QWITT diode structures examined in this study is shown in Chapter 4 (Figs. 4.1&4.3). A block diagram of both the waveguide (WR-90) and planar self oscillating mixer circuits which operate at X-band is shown in Fig. 5.6. In the waveguide circuit the QWITT diode is mounted on a micrometer controlled post which is in electrical contact with the waveguide walls. The dc bias to the device is provided using a whisker contact which is connected to a metallic post inside the waveguide. An E-H tuner is used at one end of the waveguide to minimize rf reflection and improve the conversion efficiency. The sliding short at the other end of the waveguide can also be adjusted to minimize conversion loss. For any particular value of RF input power and frequency, the E-H tuner and the sliding

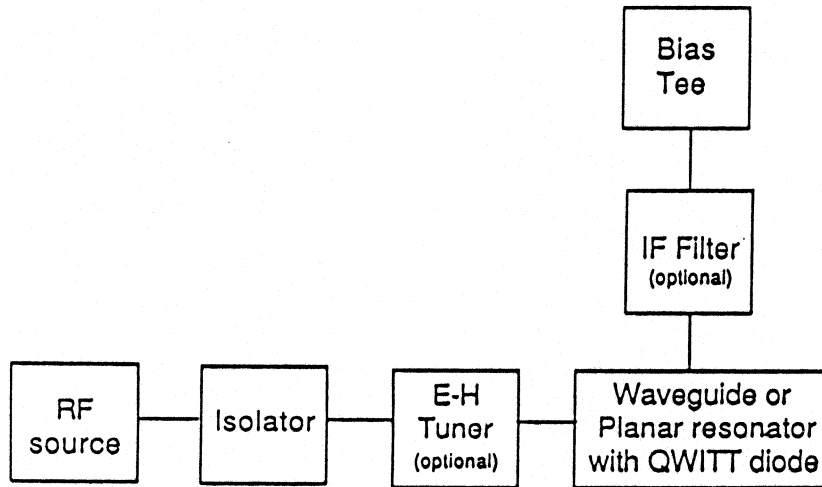


Fig. 5.6: Block diagram of both waveguide and planar self oscillating mixer circuits.

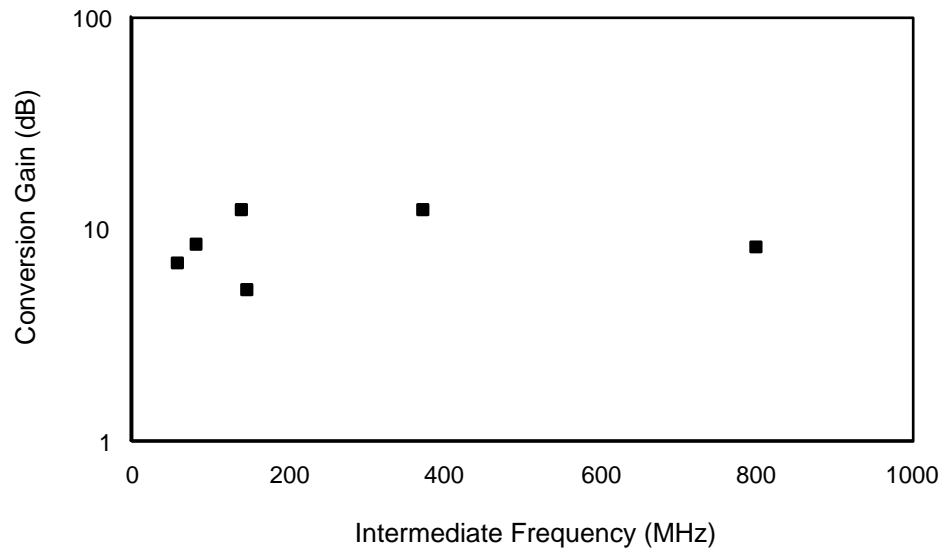


Fig. 5.7: Conversion gain as a function of the center frequency of the IF signal in the X-band waveguide self oscillating mixer using the QWITT diode.

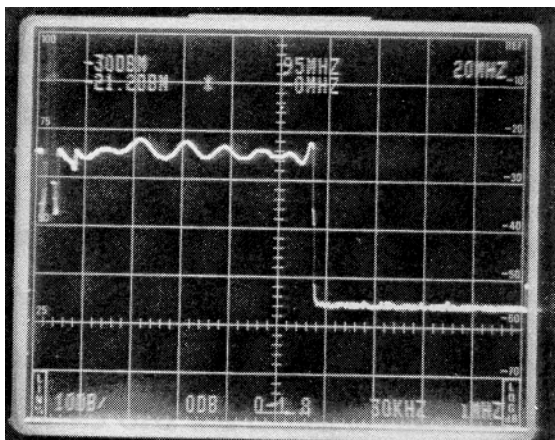


Fig. 5.8: Photograph of broadband IF signal from 2 to 100 MHz with an average power of -52 dBm. The rf signal power is -49 dBm centered at 9.3 GHz.

short are adjusted to obtain the highest power in the IF signal. The RF signal is then varied and the power in the IF signal is monitored. The bandwidth of the IF signal is set by the range of frequencies where the RF signal can be freely varied without changing the output power level of the IF signal. Hence, if the RF input frequency can be varied from 9.3 GHz to 9.4 GHz without any change in the IF signal power, that corresponds to a bandwidth of 100 MHz. The ratio of the power levels of the IF signal and RF input in this bandwidth is known as the conversion efficiency.

For use as a self-oscillating mixer, the DC bias points of the QWITT diodes were fixed at a value which produced maximum power from the QWITTs when operated as oscillators. This also sets the center frequency for operation of the self-oscillating mixer, corresponding to the free-running oscillation frequency. A typical RF input frequency of 9.3 GHz was chosen to characterize the waveguide mixer circuit. The measured IF frequency always corresponded to the difference between the known RF and free-running QWITT oscillation frequencies. In the waveguide mixer circuit using device C (see Chapter 4, Fig. 4.1), a maximum conversion gain of 10 dB was obtained over a narrow bandwidth of 10-20 MHz. The center frequency of the IF signal which results in conversion gain can be varied from the MHz range to about 1 GHz (see Fig. 5.7). If broad band operation (around 100-200 MHz) is desired this could be achieved without re-tuning the waveguide circuit using all devices, A, B, and C, with an average conversion loss of about 3-5 dB (see Fig. 5.8).

The planar self oscillating mixer uses a microstrip resonant circuit [80, 81] and operates in the fundamental conversion mode. The oscillation frequency of the mixer in this circuit was about 10 GHz. We were able to obtain conversion gains of

about 4 dB over a narrow bandwidth of 10-20 MHz. At larger bandwidths (40-200 MHz) conversion losses of about 10 dB with 1.5 dB fluctuation over the entire band were measured.

It is important to note that conversion gain in both the waveguide and planar mixer circuits was constant over a wide range in RF power level, until the RF power became comparable to the output power of the free-running QWITT diode oscillator. Although no noise measurements have been made to date, IF conversion gain has been obtained down to an RF input power of -60 dBm (10^{-9} W). While conversion loss operation was obtained from all devices used in this study, only device C, with the 2000 Å depletion region length, provided conversion gain. This may be attributed to changes in the NDR region in the I-V curve about the DC bias point causing changes in device conductance and thus affecting the efficient mixing properties of the circuit. By way of comparison, mixers using Schottky diodes are incapable of conversion gain and typically exhibit a conversion loss of 3 dB for room temperature operation at X-band. Best results for a room temperature HEMT self-oscillating mixer have demonstrated a conversion gain of 4.5 dB at X-band. Our results demonstrating a room-temperature conversion gain of 10 dB at X-band using a QWITT diode are the highest reported for a mixer circuit using any semiconductor device.

5.3 Conclusions

In this chapter microwave and millimeter wave characteristics of QWITT diode oscillators and self-oscillating mixers have been presented. An output power

of 1 mW, corresponding to an output power density of 3.5-5 kW/cm² in the frequency range of 5-8 GHz has been obtained from a planar QWITT oscillator. This is the highest output power obtained from any quantum well oscillator at any frequency and is approximately 5 times higher power and 2-3 higher output power density than reported in the literature [20] for a comparable frequency. This result also represents the first planar circuit implementation of a quantum well oscillator. By comparison, the cw output power density obtained from an IMPATT diode at these frequencies is 10-30 kW/cm². In addition, we have presented results on improving device efficiency by optimizing the design of the drift region in the device through the use of a doping spike. By optimizing the doping concentration of the spike, an increase in efficiency from 3% to 5% is obtained, without compromising on output power at X-band. Good qualitative agreement between dc and rf characteristics of QWITT devices and theoretical predictions based on small signal and large signal analyses has been obtained. Millimeter wave oscillations at 28-31 GHz in a full height waveguide circuit with an output power of 30 μW have also been obtained.

There is considerable room for optimization of both the resonant cavity and physical device parameters to maximize the oscillator output power. By choosing a InGaAs/InAlAs QWITT structure with high current densities and large peak-to-valley current ratios, even higher output power densities, comparable to an IMPATT diode, should be realizable. By appropriately choosing the thickness of the quantum well layers the peak current density can be increased further [20], thus improving the device output power. Proper device area optimization [66] will also further enhance the rf output power. It may also be possible to power combine these devices in

parallel by periodically loading a parallel plate waveguide [76, 97]. Nonetheless, the performance achieved here is promising and through further improvements in device and circuit design higher power output may be possible. It seems clear that the actual power limitations of quantum well oscillators have not yet been determined, and that through the use of QWITT design principles useful power levels may be achieved at millimeter wave frequencies.

We have shown that self oscillating QWITT diode mixers have the ability to produce conversion gain at X-band frequencies. Our waveguide mixer exhibits a conversion gain of about 10 dB in a narrow bandwidth, and a conversion loss of about 3-5 dB if broad band operation is desired. The planar mixer circuit exhibits a narrow band conversion gain of 4 dB or a broad band conversion loss of 8 dB. To the best of our knowledge this is the first report of conversion gain obtained from a self-oscillating mixer using any quantum well device and is also the highest conversion gain reported for a mixer circuit using any semiconductor device.